Journal of Civil Engineering and Construction 2023;12(3):111-125
https://doi.org/10.32732/jcec.2023.12.3.111

Numerical Modelling of Structural Behavior of RC Frames With and Without Infill Walls Subjected to Progressive Collapse

Sanjeev Bhatta[1], Jian Yang[1,2], Qing-Feng Liu[1]

1. School of Naval Architecture, Ocean and Civil Engineering, Shanghai Jiao Tong University, Shanghai, China
2. School of Civil Engineering, University of Birmingham, UK
E-mail:sanjeev.sapsan@gmail.com (Corresponding author)

Received: 2 December 2022; Accepted: 13 May 2023; Available online: 30 June 2023

Abstract: This paper aims to develop a numerical model of RC frame considering the same geometrical properties, material properties and boundary conditions in ABAQUS and validated with the experimental results comparing its force-displacement curve, damage pattern and stress and strain variations with the experimental outcomes. The use of infill walls increases the progressive collapse resistance force, mainly in the CAA. This is due to the addition of compressive action of infill walls to beam bending and CAA of RC frame. Plastic hinge was observed at the beam ends in case of RC bare frame. However, in the case of RC frame with infill wall, the plastic hinge was formed at some distance from middle joint interface and near the adjacent column joint on first floor and at some distance from adjacent column joint and near middle joint interface on second floor. Furthermore, in order to examine the effect of full height infill walls on progressive collapse resistance mechanism, RC frame with full height concrete block is modeled in ABAQUS and compare the results. It is seen that the RC frame with full height infill walls provides much higher progressive collapse resistance force in all stages i.e. beam mechanism stage, transient stage and catenary action stage.
Keywords: Infill walls; ABAQUS; Progressive collapse; Catenary action; RC frame; Finite element modeling.

1. Introduction

The term progressive collapse was not the integral part of the structural engineering before the partial collapse of Ronan point apartment in London, in 1968. The partial collapse of Ronan point is a landmark event which drew interest of structural engineering community and academic researchers for the first time towards the topic "progressive collapse". Progressive collapse is defined by the ASCE/SEI 7 [1] as "the spread of an initial local failure from element to element, which eventually results in the collapse of an entire structure or a disproportionately large part of it." The flurry of interest on research works on progressive collapse begun after the collapse of Alfred P. Murrah Federal Building in Oklahoma City, USA in 1995. In addition, the terrorist attack on World Trade Center in New York, USA, in 2001 caused large number of casualties, which raised the progressive collapse at the highest level of interest all over the world [2]. In a common progressive collapse event where a vertical element is lost, there exits three critical load resisting mechanisms – flexural action (FA) [3], compressive arch action (CAA) and catenary action (CA) [4,5]. Initially all beams are able to sustain the vertical loads through flexural action which they are design for. Compressive arch action provides additional flexural strength due to axial lateral restraint. Catenary action is the mechanism by which the structure redistributes the load carried by the failed member to the adjacent members through axial tension force induced in the bridging beams at large displacement [6]. The use of masonry infill walls in the RC frame structure is widely accepted. However, its significance on the structural resistance is often neglected considering it as a non-structural members. It is widely known that the infill walls behave as struts in frame structures, hence, it may have non-negligible effects on a structure's resistance capacity against various failure modes. The interaction between the RC frame and the infill panels was studied since the late 50's. However, understanding their interaction is not straight forward because of many governing factors associated with it such as brick materials, mortar properties, infill wall thickness, brick geometry (hollow, solid, etc.), etc.

Numerous experimental works have been carried out to investigate the performance of RC frame structures subjected to progressive collapse events. An overview of experimental works of the progressive collapse of RC structures can be found in Alshaikh et al. [7]. Alogla et al. [8] examined four RC beam-column sub-assemblages and presented a new technique to prevent progressive collapse by including additional steel bars in the middle layer of RC beams. Yu and Tan [9] have carried out experiments to investigate the impacts of seismic and non-seismic reinforcing details on the progressive collapse resistance mechanism of RC beam-column sub-assemblages.

Qian [10] used quasi-static and dynamic stress techniques to test four precast concrete beam-column assemblages. Falkowicz K. [11] examined the stability and failure analysis of thin-walled composite plate elements that have been compressed axially and weakened by cut-out. One reinforced concrete and four prestressed concrete (PC) beam-column assemblies have been built and tested in a middle-column removal scenario to examine the effects of different tendon profiles on the progressive collapse behavior of these assemblies [12]. Six RC subframes with many stories by multiple bays were created, and tested, subjected to push-down loading scenarios [13]. Wang et al. [14] performed laboratory tests on two steel beam-to-column sub-assemblages with an unsupported center column are presented. The sub-assemblages are a skeleton frame (SF) and an SLSW infilled frame (IF). Li et al. [15] used quasi-static pushdown tests to examine the behavior of three half-scaled plane frame substructures with two storeys and two spans when the first-story middle column was removed.

Different numerical methods are used to perform numerical simulation of the linear and non-linear behavior of masonry such as finite element method (FEM), discrete element method (DEM) and applied element method (AEM), and Cohesive Element Method (CEM) [24]. Liu et at. [16] developed numerical models to investigate the progressive collapse behavior of steel-FRP composite bars-reinforced 3D frame constructions. Four multi-partition concrete-filled steel tubular joints with double side-plate are examined in a progressive collapse simulation by Guo et al. [17]. Elsanadedy et al. [18] investigated the behavior of RC buildings subjected to progressive collapse events caused by blast loads. Fu et al. [19] presented numerical simulations of reinforced concrete multi-story frames in scenarios of progressive collapse. DIANA modeling software is used to model reinforced concrete frames with varying floors. To study the resistance to progressive collapse in the event of middle column failure, a finite element numerical model of infilled walls and prestressed concrete frames (IW-PC frame) is developed [20]. Using 29 reinforced concrete sub-assemblages, five different test setups, and three different test scales, EL-Ariss et al. [21] determined whether the fiber element approach is appropriate for conducting a thorough numerical investigation on the possibility of progressive collapse of reinforced concrete (RC) frame structures due to interior column exclusion. Feng et al. [22] presented a numerical analysis of the precast RC frame subassemblies' progressive collapse behavior. An effective numerical model for precast RC frame sub-assemblages subject to progressive collapse is created based on open-source finite-element software. Under a middle column removal scenario (CRS), reinforced concrete (RC) frames with concrete masonry infill walls are investigated by Yu et al. [23] using numerical models based on solid elements. Nyunn et al. [24] examined how perforated masonry walls affect the capability of multi-story reinforced concrete (RC) structures to resist progressive collapse. The analysis technique is an effective and powerful tool to study the performance of the structural element in very simple to complex loading conditions. Hence, it offers a viable alternative to costly and time-consuming experiments. Furthermore, once the model is validated, it can be redeveloped for parametric study, which is very hard to obtain by experiments. In this study, a numerical model is developed to evaluate the resistance capacities of RC frames provided with and without infill walls subjected to progressive collapse and validated with the experimental results in the literature. Furthermore, the parametric study is carried out to investigate the behavior of RC frames with half and full-height infill walls.

2. Finite element discretization of RC frame and masonry wall

The proposed model is developed considering the same geometric, material properties and boundary conditions applied in the experimental works conducted by Shan et al. [25]. Dimension and reinforcement details are as shown in Figure 1. The quasi-static loading response of this proposed model is studied using commercially available software ABAQUS. The concrete damage plasticity model available in ABAQUS is used for modeling concrete and masonry unit. For the modeling of steel reinforcement elastic-linearly plastic stress-strain behavior is adopted. RC Frame and masonry units are developed using 3D continuum elements, C3D8R, with reduced integration and hourglass control. Similarly, reinforcement in the RC frame is modeled using 3D two-nodded linear truss element T3D2. To realize the force transfer and bonding, the embedded element is applied between reinforcement and concrete. In order to develop a finite element model of masonry wall, the simplified micro-modeling approach is applied proposed by Lourenco [26]. The interaction between the masonry units as well as interfaces between masonry wall and the surrounding RC frame is modeled using the cohesive surface behavior. To simulate the transfer of shear and normal force between the masonry units and the interface between the masonry wall and the RC frame, the tangential behavior incorporating penalty friction formulation with suitable isotropic friction coefficient is used. The plasticity parameters for concrete damage plasticity adopted in this model are shown in Table 1.

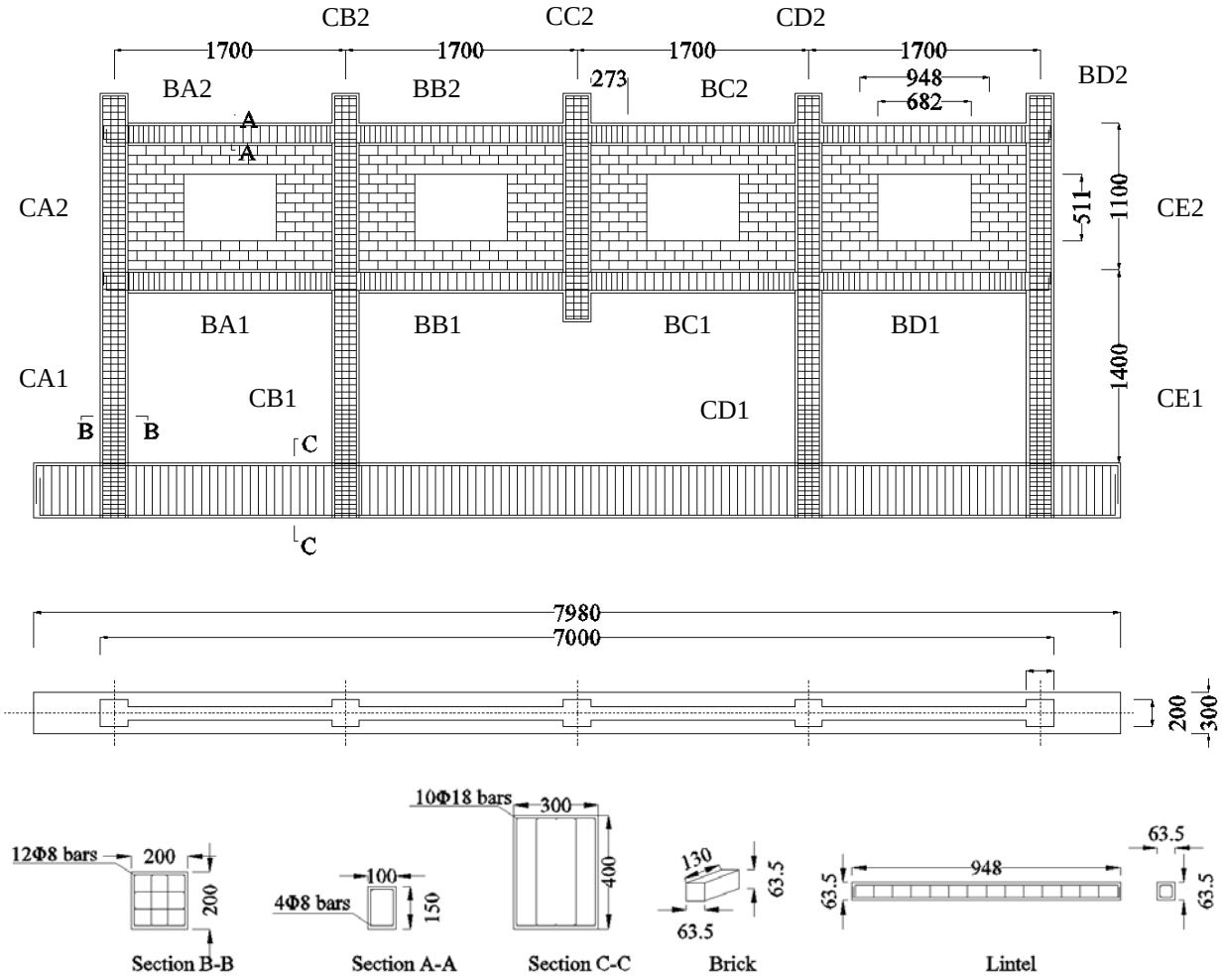

Figure 1. Dimension and reinforcement detailing [25]

Table 1. Plasticity parameters of CDP model for RC frame with and without infill walls

Parameters	Dilation Angle	Eccentricity	$\frac{\sigma_{b0}}{\sigma_{c0}}$	K_c	W_c	W_t
Values	30	0.1	1.16	0.667	1	0

To observe the performance of RC frame with infill walls, 3D models are developed in finite element software, ABAQUS. To simulate the mechanical behavior of infill wall on resisting mechanism in progressive collapse issues and perform reliable and robust analysis, various discretization schemes are adopted during the model developing process such as for the representation of reinforced concrete frame, reinforcement placed inside the concrete, material selection, interaction between concrete and reinforcement, interaction between infill walls and frame and finite element selection.

Masonry is heterogeneous and anisotropic material as because the masonry wall is composed of masonry unit, mortar, and mortar joints in vertical and horizontal directions. The key decision to model the masonry is to decide whether the masonry to modeled as a homogeneous or heterogeneous material. The masonry wall is modeled adopting simplified micro-modeling approach. In this approach, mortar joints are clamped into the mortar/masonry interface as a discontinuous element. The masonry units extended up to middle of the mortar thickness in the horizontal and vertical directions as illustrated in Figure 2 were simulated to continuum elements. Furthermore, the extended masonry unit comprises the property of masonry whereas the combined property of masonry and mortar is assigned on the interface as explained by Lourenco [26].

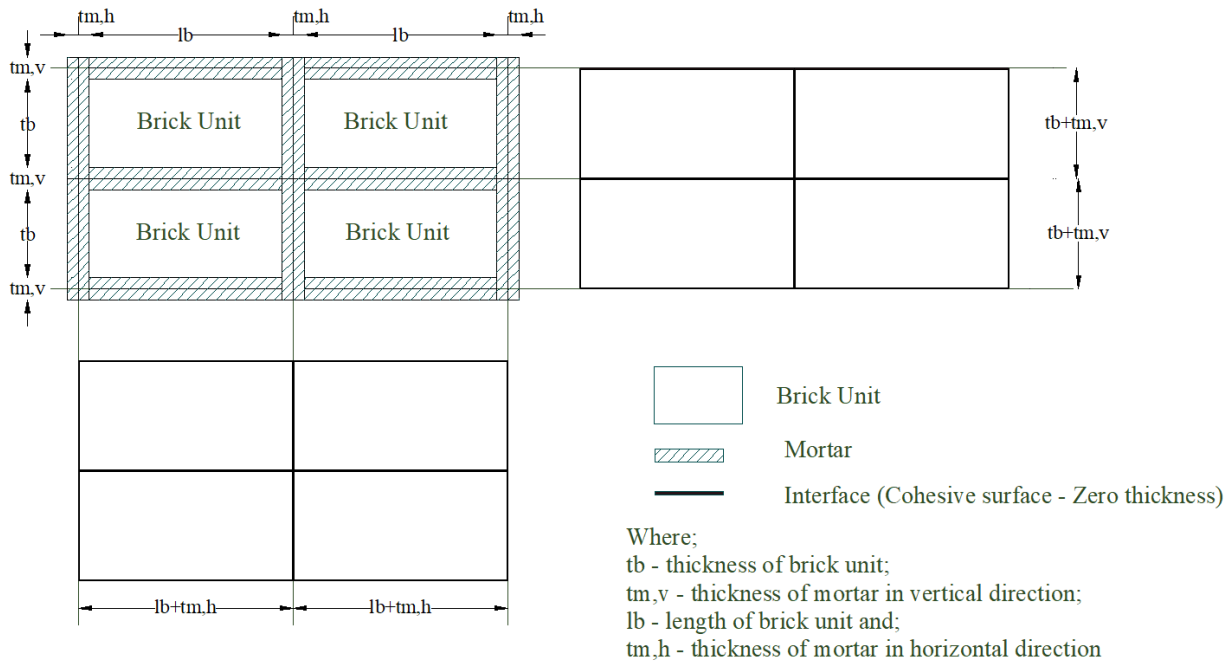

Figure 2. Simplified micro-modeling approach for masonry wall

The material model, for both the concrete and reinforcement, adopted to develop RC frame model in ABAQUS is discussed in chapter three. The interface between the masonry units involves de-cohesion and frictional contact. The rupture of interface is modeled using surface-based cohesive behavior. The de-cohesive behavior is inhibited by the traction separation. The cohesive model is combined with the friction model in order to obtain continuous transition from crack nucleation to the pure frictional stage after de-cohesion. Figure 3 shows the general scheme for modeling the contact.

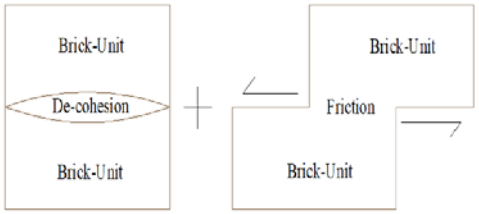

Figure 3. Combined cohesion-friction model for modeling interface

3. Material models for reinforcement and concrete

Compared with concrete, material properties of steel can be easily obtained from standard tensile test, since steel is a homogeneous material and have similar behavior in compression and tension. In this study the reinforcement bars are embedded in concrete material. The stress strain curves shown in Figure 4 are used to define steel properties. More details of the reinforcement bars used in this model are available in Table 2. Generally the Poisson's ratio of structural steel is accepted as 0.3.

ABAQUS facilitates for simulating the concrete damage using concrete damage plasticity model (CDPM). CDPM assumes tensile cracking and compressive crushing as failure mechanism in concrete. Hence CDPM will be useful to develop a proper damage simulation model for analyzing any RC structures under both static and dynamic loading [27]. In this study this technique is applied to represent complete inelastic behavior of concrete both in compression and tension along with damage characteristics. The detail of material properties of concrete is available in Table 3. The complete stress-strain compressive curve of concrete is derived using [28] model as shown in Figure 5 and tensile curve is developed using [29] as shown in Figure 6.

Table 2. Material Properties of Steel Reinforcement

Bar type	Yield strength f_y (MPa)	Elastic modulus E_s (MPa)	Strain at the start of hardening ϵ_{sh} (%)	Tensile strength f_u (MPa)	Ultimate strain ϵ_u (%)
R6	349	199,177	-	459	-
T10	511	211,020	2.51	622	11.00
T13	494	185,873	2.66	593	10.92
T16	513	184,423	2.87	612	13.43

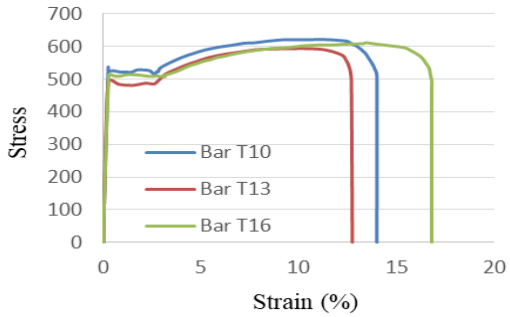

Figure 4. Stress-strain curve

Table 3. Properties of concrete

Material	Initial modulus of elasticity, GPa	Compressive strength, MPa	Tensile strength, MPa
Concrete	29.6	38.2	3.5

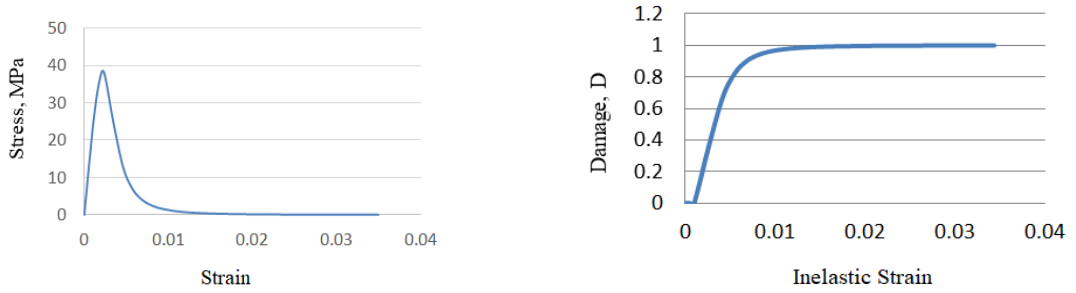

(a) (b)

Figure 5. (a) Compressive Stress-strain relationship (b) Damage vs. inelastic strain

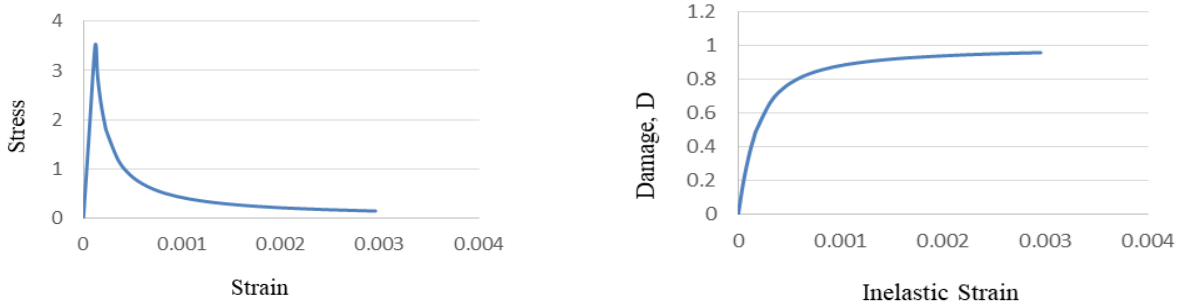

(a) (b)

Figure 6. (a) Tensile Stress-strain relationship (b) Damage vs. inelastic strain

4. Model validation

The numerical model is validated by comparing the numerical simulation results with the experimental results reported by Shan et al. [25]. The finite element model of RC frame with infill wall is developed in ABAQUS. Figure 7 shows that the force versus middle joint displacement curves obtained from numerical modeling of RC frame with and without infill walls are in good agreement with the test results in all three phases of progressive collapse resistance i.e., flexural, CAA and catenary action and the course of development of applied load obtained from numerical modeling and experiment is similar. The numerical model is validated by comparing the force-displacement curves, damage patterns and stress and strain transfer mechanisms.

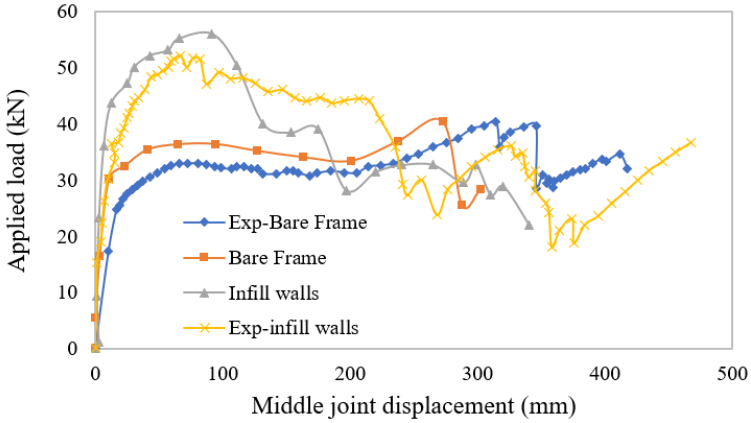

Figure 7. Applied load versus middle joint displacement

Figure 7 represents the curves of force versus displacement of the middle column for bare frame in middle column removal scenario. The numerical modeling results for the bare frame shows that maximum resistance force of 36.38 KN is attained at the vertical displacement of 94.3 mm in the compressive stage. The curve descends after the attaining the peak load until the end of the compressive stage. At this stage it is observed that resistance force of 33.39 KN is obtained corresponding to the vertical displacement of 201.06 mm. The further increase in resistance force in the curve indicates the development of catenary action in the later stage.

Figure 7 also represents the curves of force versus displacement of the middle column for infilled frame in middle column removal scenario. The higher resistance force is observed in the compressive stage as compared with the bare frame as shown in Table 4. It shows that the resistance force achieved its maximum value of 56.06 KN at a vertical middle joint displacement of 91.57 mm. The curve then descends up to the vertical displacement of 196.82 mm with the resistance force of 28.19 KN. The further increased in resistance force after 196.82 mm displacement shows the activation of the catenary action.

Table 4. Numrical modeling results

Numerical RC Specimens	Peak Load at CAA		Beginning of CA		Catenary Stage	
	Max. Load, KN	MJD mm	Load KN	MJD mm	Max. Load KN	MJD mm
Bare Frame	36.38	94.3	33.39	201.06	40.36	272.9
Infilled Frame	56.06	91.57	28.19	196.82	32.35	295.39

4.1 Development of cracks in bare frame

Figure 8 explains that the development of cracks at three stages of collapse mechanism. Firstly, few cracks were observed at the ends of beams in bays B and C as shown in Figure 8 (a) at the end of initial stage. At maximum compressive stage, this cracks further developed but they still concentrated in regions near the beam ends as illustrated in Figure 8 (b). Furthermore, these cracks continued to widen and extend until the end of compressive stage. As shown in Figure 8 (c), even in the catenary action the cracks are continually widen and concentrated in regions near the beam ends in bay B and C. It also shows that there is very little or no damage to beam in bays A and D. It was observed that the top longitudinal rebar in the beam yielded near the adjacent column of bay B and C and bottom rebar yielded occurred in regions near the middle column joint interface as shown in Figure 9.

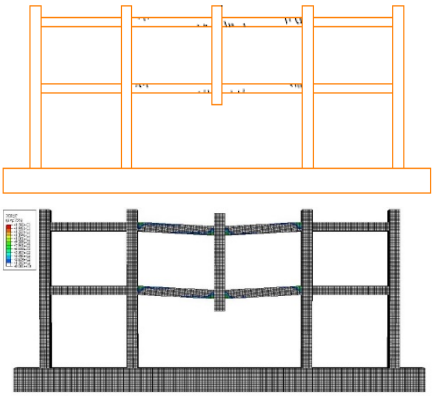

a) At maximum initial stage (i) Experiment [25] (ii) Numerical modeling

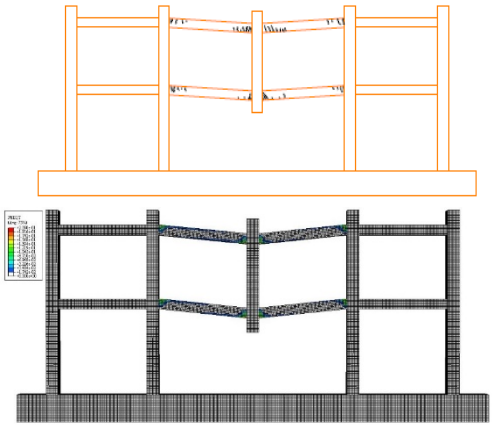

b) At maximum compressive stage (i) Experiment [25] (ii) Numerical modeling

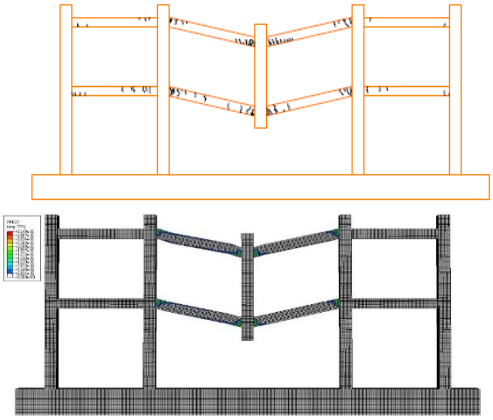

c) At maximum catenary stage (i) Experiment [25] (ii) Numerical modeling

Figure 8. Development of cracks in bare frame

4.2 Development of cracks in bare infilled frame

The RC frame with infill wall shows the different crack formation process than RC frame without infill wall. It is observed that in the initial stage, at a vertical displacement of 14.19mm, the cracks in the beam and diagonal major cracks were concentrated in the openings of infill walls. With the increase in vertical displacement, these cracks gradually widened in the later stages and only a few secondary cracks were observed in the weak positions around the major cracks in the infill walls. Figure 10 shows the development of crack formation in the beam and infill walls at the end of three stages; initial stage, compressive stage and catenary stage. It is observed that in the end of catenary stage, the cracks in the beam were concentrated in the beam ends and major cracks observed in the infill walls near the corner of openings.

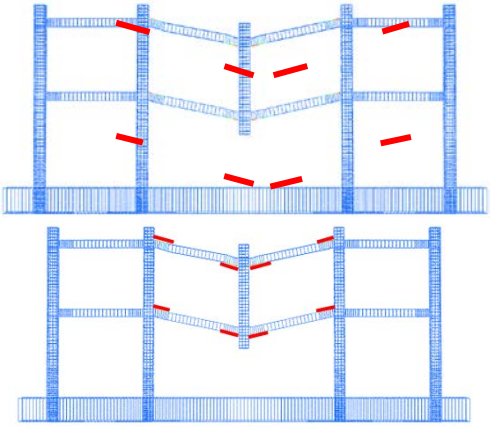

Figure 9. Locations of rebar yielding in bare frame

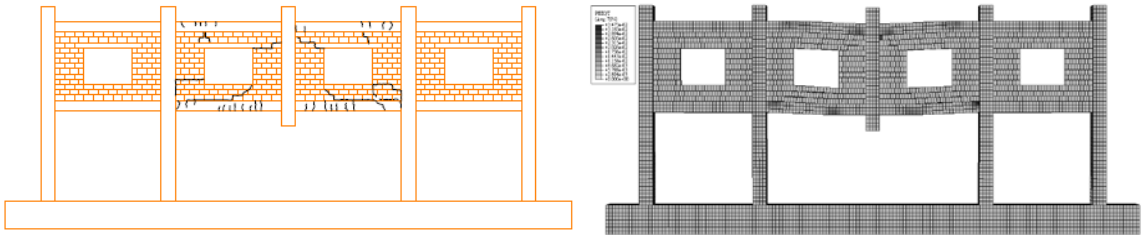

a) At maximum initial stage (i) Experiment [25] (ii) Numerical modeling

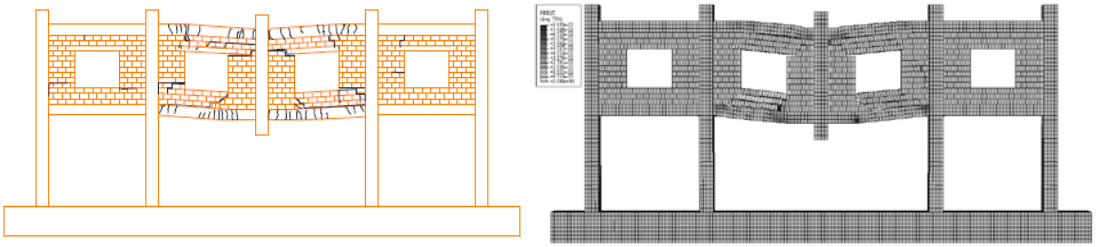

b) At maximum compressive stage (i) Experiment [25] (ii) Numerical modeling

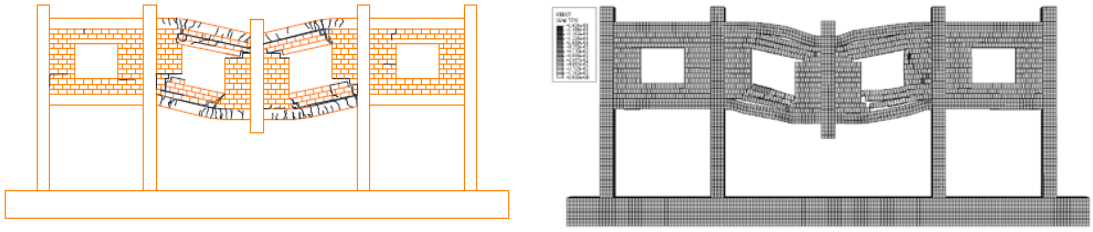

c) At maximum catenary stage (i) Experiment [25] (ii) Numerical modeling

Figure 10. Development of cracks in infilled frame

5. Strain variation, axial stress and horizontal displacement versus middle joint displacement

5.1 Strain variation in bare frame

Figure 11 shows the strain variation in reinforcement in the double span beam of RC bare frame near adjacent column joint and column removal joint after the middle column has been removed. It shows that the top bar of beams near BC1-CD1 and BB1-CB1 joints and bottom bar of beams near middle column joint interface on first and second floor are always in tension. Likewise, the bottom bar of beams near adjacent column joint interface and top bar of beams near middle column joint interface on first and second floor are always in compression. The strain in top and bottom rebar along the different position of beam as plotted in Figure 12 further illustrates the top bar near adjacent column joint interface and bottom bar near column removal joints are always in tension.

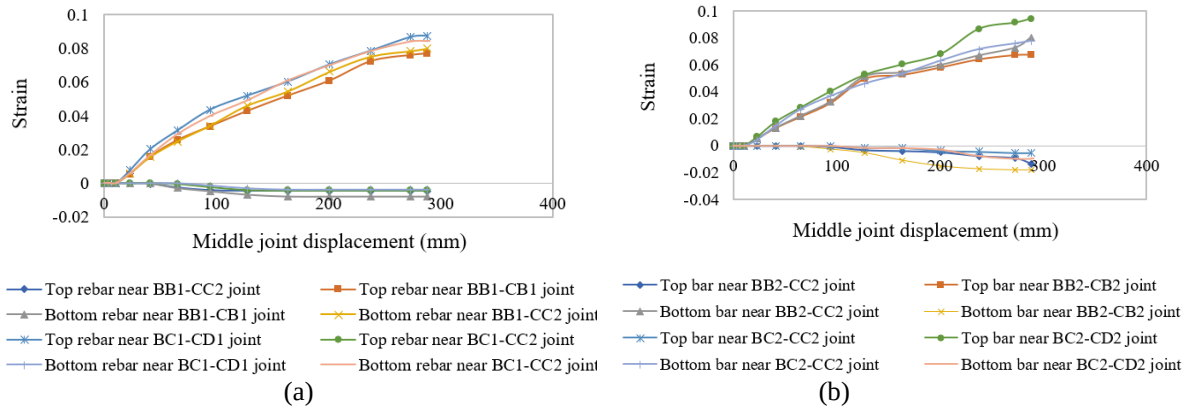

(a) (b)

Figure 11. Strain variation in rebar near beam column joints on the (a) first floor (b) second floor of bare frame

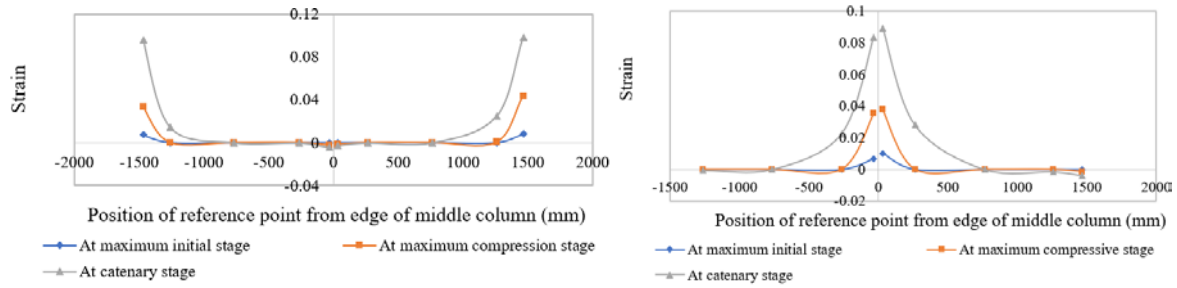

(a) (b)

Figure 12. Strain variation in (a) top bar (b) bottom bar of double span beam (BB1-BC1) of bare frame

5.2 Strain variation in infilled frame

Figure 13a shows the strain variation in top bar of double span beam (BB1-BC1) of RC frame with infill wall after the middle column has been removed. It is seen that the strain in top bar near the adjacent columns are higher than the strain in top bar near column removal joint. It also shows that the strain in top rebar of beam BC1 is higher at some distance right from the middle joints and at some distance left from the middle column joints in case of BB1. Similarly, Figure 13b, which is a plot of strain variation in bottom bar of double span beam (BB1-BC1) of infilled frame after column loss, shows that the strain in bottom rebar of beam BB1 is higher at some distance left from the middle joints and at some distance right from the middle joint in case of BC1. From this it can be said that, unlike the bare frame, the plastic hinge are formed at some distance from middle column joint and near adjacent column in case of infilled frame, Figure 15b.

The curve obtained by plotting strain in top rebar of beam BB2 and BC2 as in Figure 14a. It is observed that the strain is higher at some distance right from adjacent column joints in the beam BB2 and at some distance left from adjacent column in case of beam BC2. Similarly, Figure 14b shows that the strain in bottom bar is higher at the middle joint interface in case of both the beam BB2 and BC2. From this, it can be said that plastic hinge are formed at some distance from adjacent column joints and near the middle column joint in the beam at second story, Figure 15b. The position in beam top and bottom rebar having higher strain is shown in Figure 15a.

5.3 Axial stress versus middle joint displacement in bare frame

The plot of axial stresses of beam longitudinal bar with middle joint displacement, Figure 16a illustrates that the bottom bar at the left end and the top bar at the right end of beam BC1 are always in tension. It is also seen that the middle portion of the longitudinal bar was in compression and changed into tension the maximum compressive stage. Furthermore, the left end top bar and the right end bottom bar of beam BC1 was in compression and changed into tension after the initiation of the catenary stage. The plot of axial stress and middle joint displacement in Figure 16b shows that the left bar of the column CD1was in tension and changed into compression, whereas, the right bar of the column CD1was in compression and changed into tension after the initiation of catenary action. This illustrates that initially there was outward horizontal movement of the column in the compressive stage and inward horizontal movement of the column in the catenary action stage.

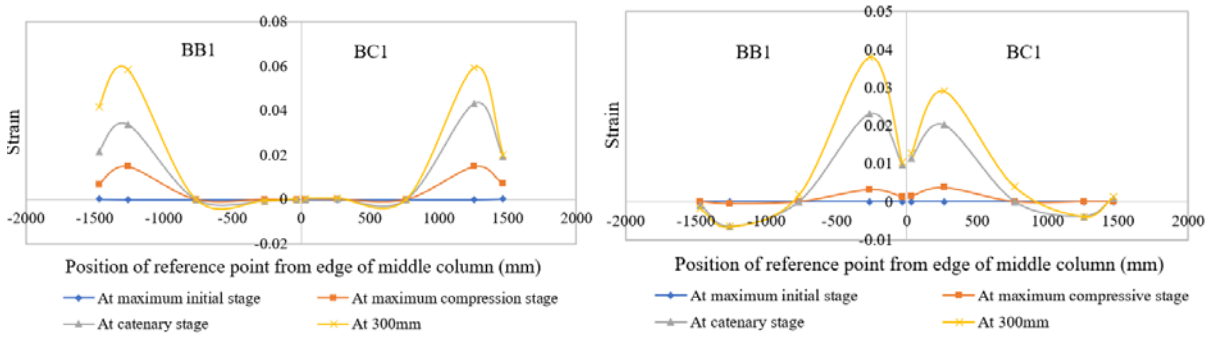

(a) (b)

Figure 13. Strain variation in (a) top bar (b) botton bar of double span beam (BB1-BC1) of infilled frame

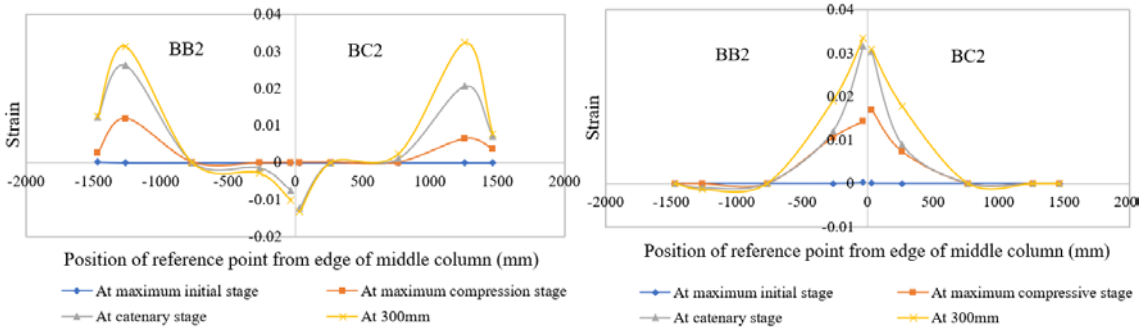

(a) (b)

Figure 14. Strain variation in (a) top bar (b) bottom bar of double span beam (BB2-BC2) of infilled frame

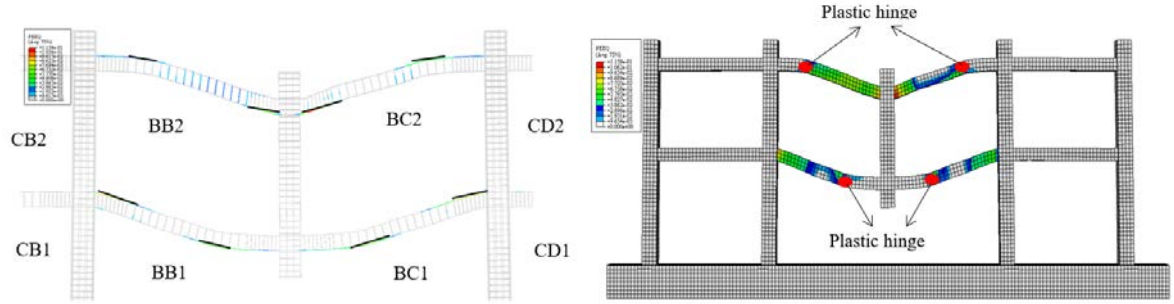

Figure 15. Location of (a) higher strain in rebar (b) plastic hinges in beam in case of infilled frame

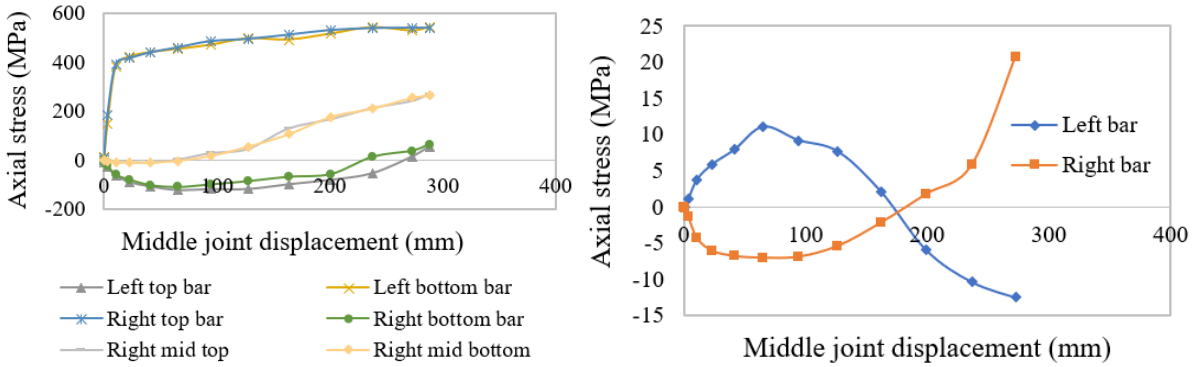

a) Beam BC1 (b) Column CD1

Figure 16. Axial stress variation in beam and column of bare frame

5.4 Axial stress versus middle joint displacement in bare frame

Figure 17a shows the stresses in longitudinal bar of beam BC1 with respect to displacement. It illustrates that the right top bar and left bottom bar are always in tension. It is observed that the bottom bar at the middle of beam BC1 is also in tension throughout the numerical analysis. However, the rebar at the top of middle and bottom of the right end were in compression and changes into tension in the catenary stage. Also, the left top bar of beam BC1 was in compression and changed into tension after the completion of compressive stage.

The plot of axial stress versus the middle joint displacement of column CD1 in Figure 17b shows that the left longitudinal bar was in tension and right longitudinal bar was in compression in the compressive stage. However, the left bar changed into compression and right bar changed into tension after the commencement of catenary action. Hence, this proves that initially there was outward movement of column in the compressive stage and the column moved inward in the catenary action stage. This is also further illustrated by plotting middle joint displacement versus horizontal displacement.

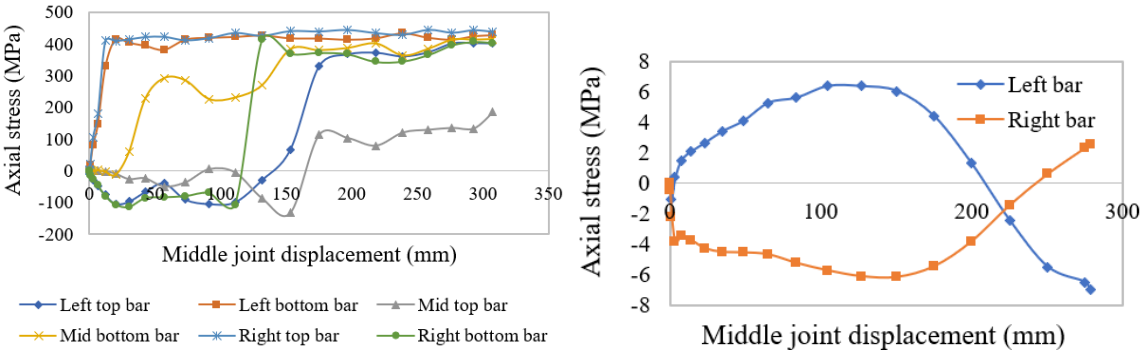

a) Beam BC1 (b) Column CD1

Figure 17. Axial stress variation in beam and column of infilled frame

5.5 Middle joint displacement versus horizontal displacement

Figure 18a is the plot of horizontal displacement of adjacent column joint and exterior column joint versus the middle joint displacement after column loss in case of bare frame. It is observed that the adjacent column moved outward in the compressive stage and received maximum outward horizontal displacement of 3.95mm at vertical displacement of 94.3mm. After it reached to maximum, the horizontal displacement then starts decreasing and becomes zero at vertical displacement of 205mm in case of CB2-BB2 joint. The inward movement of adjacent column is observed after the catenary stage is initiated. The similar case is observed in the exterior column of bare frame as shown in Figure 18b. Considering CA1-BA1 joint, the maximum outward horizontal is obtained as 4.15mm at vertical displacement 106.11mm. The exterior column joint comes to the initial position at vertical displacement of 201.06mm.

The plot of horizontal displacement of adjacent column joint and exterior column joint versus the middle joint displacement after column loss in case of infilled frame is shown in Figure 19. It is observed that the horizontal movement of adjacent and external column joints is larger in infilled frame than bare frame. The Initially, the horizontal movement of the adjacent column is observed outward and reached maximum of 5.76mm at vertical displacement of 91.57mm in case of CB2-BB2 joint, Figure 19a. The movement has changed from outward to inward after vertical displacement of 196.82mm. Similarly, from Figure 19b, considering CA1-BA1 joint for exterior column joint case, the maximum outward movement of 5.04mm is observed in compressive stage at vertical displacement of 91.57mm. The catenary stage is activated at vertical displacement of 218.24mm where it is observed that the outward horizontal movement of exterior column joint has changed into inward movement.

6. Effect of full-height infill walls

To investigate the effect of full height infill wall on progressive collapse resistant mechanism, a 3D explicit model is developed in ABAQUS. To develop this model Figure 21, a homogeneous block assigned with masonry properties is considered, from Shuang Li et al. [30], instead of full height masonry wall. The cohesive behavior is adopted to define the interaction between the frame and the infill block. The plot of applied load versus middle joint displacement as shown in Figure 20 illustrates the good agreement of finite element results with that of experimental results. Figure 20 also explains the sensitivity of mesh size in the analysis. Initially, it is seen that adjacent and external column joints moved horizontally outward in the compressive stage and later changed into inward movement in the catenary stage which is illustrated by Figure 22. The FEM results shows that the strain are concentrated more near the center column joint and at some distance from adjacent column in the beam of

second floor (BB2-BC2). However, very less strain is observed near column removal joint and higher near the adjacent column joint in the beam of first floor (BB1-BC1). Hence, it can be said that, unlike the bare frame, plastic hinge are formed at some distance from middle column joint and near the adjacent column joint in case of beam on first floor whereas plastic hinges are formed at some distance from adjacent column joints and near the middle column joint in case of beam on second floor.

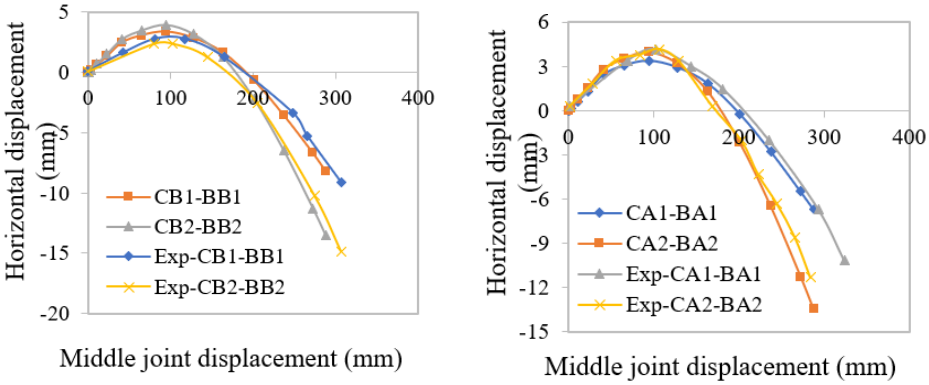

Figure 18. Bare frame a) Adjacent column joints b) Exterior column joints

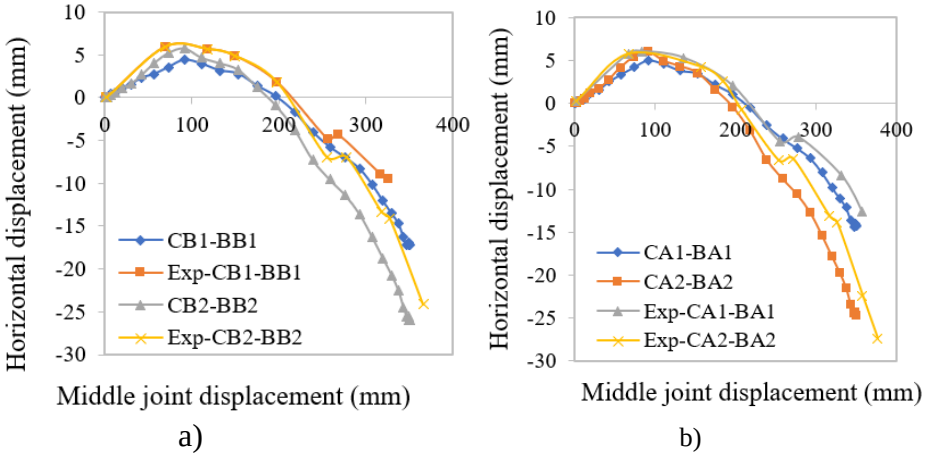

Figure 19. Infilled frame a) Adjacent column joints b) Exterior column joints

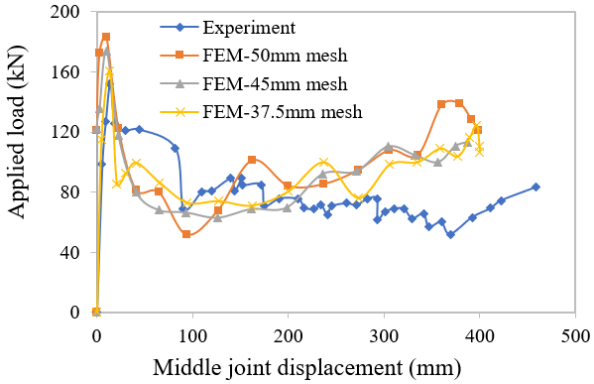

Figure 20. Applied load versus middle joint displacement in case of RC frame with full-height infill wall

The plot of applied load versus the middle joint displacement obtained from finite element analysis results for the RC bare frame, RC frame with infill walls with opening and RC with full-height infill walls are shown in Figure 23. On comparison, it is observed that RC frame provided with the infill walls with opening provides maximum resistance in the compressive stage. However, RC frame provided with full-height infill walls provides much larger progressive collapse resistance force in overall. It is seen that the the resistance force is provided by beam bending and CAA in case of bare frame. However, in case of frame provided with infill walls with opening

the compressive infill walls action added more resistance force due to which higher resistance force is obtained in the compressive stage and the full-height infill wall provided the much higher structural resistance in all stages of progressive collapse mechanism.

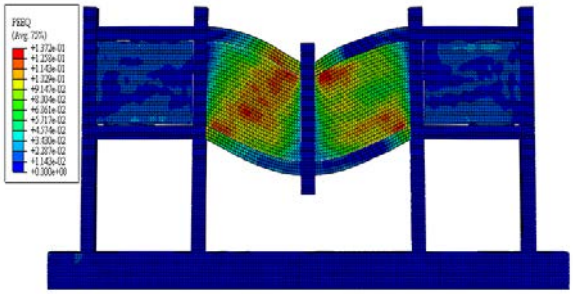

Figure 21. Numerical modeling results in case of RC frame with full-height infill walls

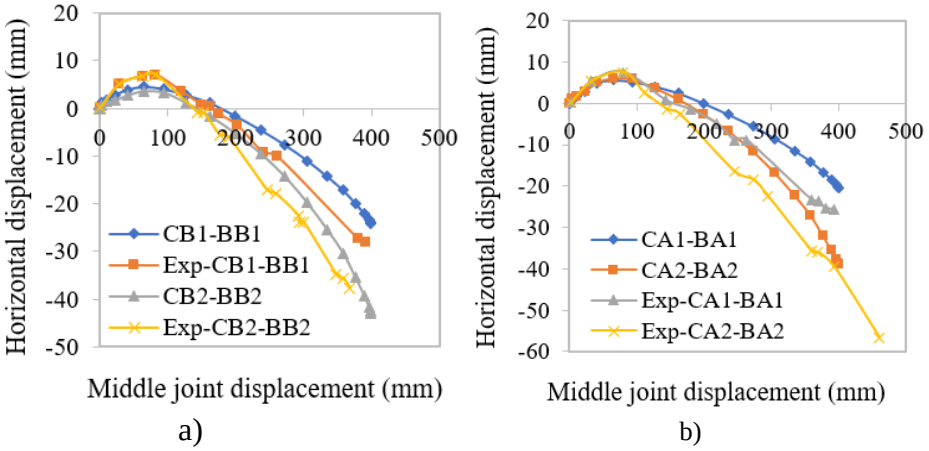

Figure 22. Full-height Infilled frame a) Adjacent column joints b) Exterior column joints

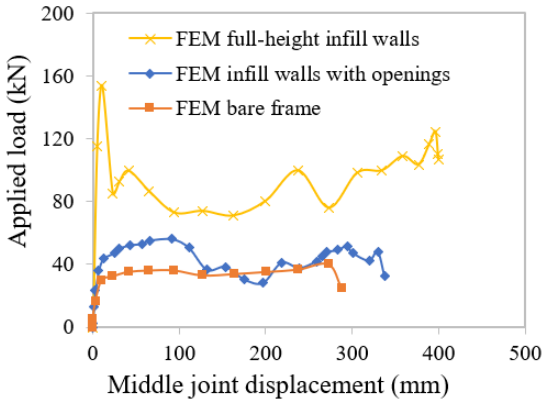

Figure 23. Applied load versus middle joint displacement comparison curve

7. Conclusions

1) A simplified model is developed to investigate the structural behavior of RC beam column frames under a middle column removal scenario and its reliability is verified by experimental results in literature. Therefore, the proposed model is able to predict the capacity of structural resistance to collapse at beam mechanism stage and catenary action stage with satisfactory accuracy.

2) In the case of bare frame, resistance force is provided by beam bending and CAA in the compressive stage, whereas, in case of infilled frame, the compressive infill wall action added more resistance force due to which higher resistance force is obtained in the compressive stage of applied load versus middle joint displacement curve of infilled frame.

3) For RC frame provided with infill walls with opening, initially the cracks were observed in the beam and diagonal major cracks were concentrated in the openings of infill walls. With further increase in vertical

displacement, these cracks gradually widened in the later stages and only a few secondary cracks were seen in the weak regions around the major cracks in the infill walls.

4) The plastic hinges in RC bare frame was are observed in the beam ends whereas plastic hinge are formed in the beam at some distance from middle column joint and near the adjacent column joint on first floor and similarly, at some distance from adjacent column joints and near the middle column joint of beam on second floor in the case of RC frame with infill wall.

5) Comparing RC bare frame, RC frame with infill wall with opening and RC frame with full-height infill wall, the RC frame provided with masonry wall with opening has the higher resistance to progressive collapse in the compressive stage as compared with bare frame. However, much larger progressive collapse resistance force in overall is obtained in case of frame with full-height infill wall.

8. References

[1] ASCE/SEI. Minimum design loads for buildings and other structures. ASCE/SEI 7, Reston, VA, 424. 2010.
[2] Azim I, Yang J, Bhatta S, Wang F, Liu QF. Factors influencing the progressive collapse resistance of RC frame structures. Journal of Building Engineering. 2020;27:100986.
[3] Stinger SM, Orton SL. Experimental Evaluation of Disproportionate Collapse Resistance in Reinforced Concrete Frames. ACI Structural journal. 2013;110(3).
[4] Fascetti A, Kunnath SK, Nisticò N. Robustness evaluation of RC frame buildings to progressive collapse. Engineering Structures. 2015;86:242-249.
[5] Su Y, Tian Y, Song X. Progressive collapse resistance of axially-restrained frame beams. ACI Structural Journal. 2009;106(5).
[6] (GB50010-2010)[S]. Code for design of concrete structures. China Architecture and Building Press. 2010.
[7] Alshaikh IM, Bakar BA, Alwesabi EA, Akil HM. Experimental investigation of the progressive collapse of reinforced concrete structures: An overview. In:Structures 2020 (Vol. 25, pp. 881-900). Elsevier.
[8] Alogla K, Weekes L, Augusthus-Nelson L. A new mitigation scheme to resist progressive collapse of RC structures. Construction and Building Materials. 2016;125:533-545.
[9] Yu J, Tan KH. Experimental and numerical investigation on progressive collapse resistance of reinforced concrete beam column sub-assemblages. Engineering Structures. 2013;55:90-106.
[10] Qian K, Liang SL, Xiong XY, Fu F, Fang Q. Quasi-static and dynamic behavior of precast concrete frames with high performance dry connections subjected to loss of a penultimate column scenario. Engineering Structures. 2020;205:110115.
[11] Falkowicz K. Experimental and numerical failure analysis of thin-walled composite plates using progressive failure analysis. Composite Structures. 2023;305:116474.
[12] Huang Y, Tao Y, Yi W. Progressive collapse behavior of prestressed concrete frames with various tendon profiles. Journal of Building Engineering. 2023:106631.
[13] Qian K, Li B. Effects of masonry infill wall on the performance of RC frames to resist progressive collapse. Journal of Structural Engineering. 2017;143(9):04017118.
[14] Wang F, Yang J, Wang XE, Azim I. Study on progressive collapse behaviour of steel-framed substructures with sheathed CFS stud infill walls. Journal of Building Engineering. 2021;42:102720.
[15] Li ZX, Liu H, Shi Y, Ding Y, Zhao B. Experimental investigation on progressive collapse performance of prestressed precast concrete frames with dry joints. Engineering Structures. 2021;246:113071.
[16] Liu XY, Qin WH, Xu ZD, Xi Z, Zhang ZC. Investigation on the progressive collapse resistance of three-dimensional concrete frame structures reinforced by steel-FRP composite bar. Journal of Building Engineering. 2022;59:105116.
[17] Guo L, Gao S, Mu C. Behaviour of MCFST column-steel beam connection with side plates in the scenario of column loss. Journal of Constructional Steel Research. 2020;171:106150.
[18] Elsanadedy H, Khawaji M, Abbas H, Almusallam T, Al-Salloum Y. Numerical modeling for assessing progressive collapse risk of RC buildings exposed to blast loads. InStructures 2023 (Vol. 48, pp. 1190-1208). Elsevier.
[19] Fu QL, Tan L, Long B, Kang SB. Numerical Investigations of Progressive Collapse Behaviour of Multi-Storey Reinforced Concrete Frames. Buildings. 2023;13(2):533.
[20] Chang D, Zeng B, Huang LJ, Zhou Z. Investigation on progressive collapse resistance of prestressed concrete frames with infilled walls. Engineering Failure Analysis. 2023;143:106866.
[21] El-Ariss B, Elkholy S, Shehada A. Benchmark numerical model for progressive collapse analysis of RC beam-column sub-assemblages. Buildings. 2022;12(2):122.
[22] Feng DC, Wu G, Lu Y. Numerical investigation on the progressive collapse behavior of precast reinforced concrete frame subassemblages. Journal of Performance of Constructed Facilities. 2018;32(3):04018027.

[23] Yu J, Gan YP, Wu J, Wu H. Effect of concrete masonry infill walls on progressive collapse performance of reinforced concrete infilled frames. Engineering structures. 2019;191:179-193.
[24] Nyunn S, Wang F, Yang J, Liu QF, Azim I, Bhatta S. Numerical studies on the progressive collapse resistance of multi-story RC buildings with and without exterior masonry walls. InStructures 2020 (Vol. 28, pp. 1050-1059). Elsevier.
[25] Shan S, Li S, Xu S, Xie L. Experimental study on the progressive collapse performance of RC frames with infill walls. Engineering Structures. 2016;111:80-92.
[26] Lourenço PJ. Computational strategies for masonry structures. Ph.D. dissertation, University of Techology, Delft, The Netherlands. 1996.
[27] Abaqus User Manual. Abaqus Version 6.8. 2008.
[28] Popovics S. A numerical approach to the complete stress-strain curve of concrete. Cement and concrete research. 1973;3(5):583-599.
[29] Belarbi A, Zhang LX, Hsu TT. Constitutive laws of reinforced concrete membrane elements. In: Sociedad Mexicana de ingenieria sismica in world conference on earthquake engineering. 1996. p. 1-8.
[30] Li S, Shan S, Zhai C, Xie L. Experimental and numerical study on progressive collapse process of RC frames with full-height infill walls. Engineering Failure Analysis. 2016;59:57-68.